Nuclear Materials and Energy 29 (2021) 101080

Contents lists available at ScienceDirect

Nuclear Materials and Energy

journal homepage: www.elsevier.com/locate/nme

Application of a newly developed radial directional electron probe to the edge unidirectional electron current measurement in EAST

S.C. Liu [a,*], Y. Liang [a,b], N. Yan [a,*], L. Liao [a,c], W.Y. Wei [a,c], L.Y. Meng [a,c], L. Chen [a], S. Xu [b], N. Zhao [d], R. Chen [a], G.H. Hu [a], Y.L. Li [a], X.J. Liu [a], T.F. Ming [a], Y. Sun [a], J.P. Qian [a], L. Zeng [a], G. Q. Li [a], L. Wang [a], G.S. Xu [a], X.Z. Gong [a], X. Gao [a], East Team

[a] Institute of Plasma Physics, Chinese Academy of Sciences, Hefei 230031, Peoples Republic of China
[b] Forschungszentrum Jülich GmbH, Institut für Energie- und Klimaforschung – Plasmaphysik, Partner of the Trilateral Euregio Cluster (TEC), 52425 Jülich, Germany
[c] University of Science and Technology of China, Hefei 230026, Peoples Republic of China
[d] School of Science, Southwest University of Science and Technology, Mianyang 621010, Peoples Republic of China

ARTICLE INFO

Keywords:
Unidirectional electron
SOL current
Directional electron probe
Lower hybrid wave
Tokamak
Plasma

ABSTRACT

A newly developed radial directional electron probe (DEP) has been applied to the unidirectional electron current measurement on EAST tokamak. The DEP consists of two radial arrays of channels which have opposite directions and align along the local magnetic field line. Each radial array has 6 holes with a radial interval of 5 mm. Every channel has a hole with 0.5 mm radial width, 3 mm depth and 15° poloidal opening angle. The graphite collector embedded inside the hole is biased to positive potential to repel low energy ions, and high energy ions are blocked by the hole surface because their Larmor radii are larger than the radial width of hole. In consequence, the ion current collected by the DEP collector can be ignored in contrast with the electron current, as demonstrated by the *I-V* characteristics in a DEP commissioning experiment. The difference of collected current between two opposite channels signifies the unidirectional electron current in the flux tube. In a lower hybrid wave (LHW) modulation experiment, the amplitude and radial structure of unidirectional electron current induced by LHW is measured directly by this radial DEP array, and the LHW filament current covers over 20 mm radial region with a maximum of 20 A/cm^2.

Introduction

Filament current is a general phenomenon in the edge plasma of tokamaks [1] and stellarators [2]. Usually the so-called blob (filament) plays an important role in the edge cross-field transport, since a large amount of plasma is ejected into the far scrape-off layer (SOL) by this intermittency event [3]. Edge filament currents are also observed during the eruption of some plasma instabilities, such as the edge localized mode (ELM) [4]. Because the electron parallel velocity is much higher than the ion parallel velocity due to their large mass difference, the filament current is considered to be driven mainly by electrons [3,5]. The type-I ELM filament current density could be up to 4.5 MA/m^2 in ASDEX Upgrade, and a corresponding current 1.4 kA for 1 cm radius filament [6,7]. The electrons could contribute significantly to this large and unidirectional parallel SOL current [7]. Radio frequency (RF) waves can drive considerable parallel current which is mainly carried by the fast electrons in tokamak plasma [8]. For example, lower hybrid current drive (LHCD) is an efficient method to drive plasma current and control current profile, as reported in many tokamaks [9–13]. In Alcator C-Mod, the SOL current induced by LHCD could be enhanced to 20 kA in high line-averaged density discharges, indicating a large amount of lower hybrid waves (LHWs) are absorbed in the SOL rather than inside the separatrix [14]. In EAST, strong mitigation of edge localized mode (ELM) has been achieved by the LHW modulation [15], and the edge magnetic topology change induced by the SOL LHW current is proposed as a possible mechanism [16,17]. Therefore, it is very meaningful to directly measure the edge electron current, which could benefit the physical understanding of edge plasma transport, instability dynamics and current drive.

Usually, the SOL current can be estimated by the magnetic pick-up coils [6] and the retarding field analyzer (RFA) [18]. The magnetic coils located at the vacuum wall are far from the SOL current, which is

* Corresponding authors.
E-mail addresses: shaocheng.liu@ipp.ac.cn (S.C. Liu), yanning@ipp.ac.cn (N. Yan).

https://doi.org/10.1016/j.nme.2021.101080
Received 26 May 2021; Received in revised form 28 September 2021; Accepted 7 October 2021
Available online 8 October 2021

difficult to measure the structure of filaments. If the magnetic coils are mounted on the fast manipulator, it is possible to obtain the radial structure of SOL current when the coils approaching the current. The RFA can measure the distribution of ion or electron velocity inside the SOL current, but the estimated amplitude of SOL current is sensitive to the transmission of grid sheets [18,19]. Evolved from the RFA, some electron energy analyzers have been developed to measure the super-thermal electron flow and temperature [20–22]. Herein we will introduce a newly developed directional electron probe (DEP), which is able to measure the amplitude and structure of the SOL electron current with high temporal resolution. This paper will be organized as follows. Section 2 describes the setup of DEP. Commissioning and preliminary experimental results of DEP are given in section 3. Section 4 is a summary.

Setup of directional electron probe

Directional probe, consisting of two collectors located on the two sides of a central insulator, has been applied to the measurements of parallel ion flow and floating potential in the magnetically controlled plasmas [23–28]. Herein we propose a new type of directional probe which has the capability to measure parallel electron current, and consequently this new probe is named as directional electron probe (DEP). The primary difference between the traditional directional probe and DEP is that the collector of DEP is embedded inside a small and deep hole. The exploded drawing of DEP is shown in Fig. 1 (a). The DEP consists of an outside boron nitride cover, an internal ceramic holder, Langmuir probe (LP) components and directional electron probe components. The Langmuir probe components are similar with the usual probes, including front graphite tips, lead-in copper pipes and wires. The directional electron probe components include graphite collectors, copper connectors and wires. Note that the graphite collector (or LP tip) and copper connector (or LP pipe) are connected by screw thread, while the copper connector (or LP pipe) and wire are crimped together by a wire crimper which could sustain much higher temperature than soldering. As illustrated in Fig. 1 (a) and Fig. 2, the DEP graphite collector has a fan-shaped front surface which fits the inner wall of boron nitride cover, and has an L-shape back surface which plugs into the ceramic holder, in consequence the DEP graphite collector is fixed after assembly. In the boron nitride cover, there are two radial arrays of holes which have opposite directions, and the connection line of two opposite holes aligns with the local magnetic field. Each radial array has 6 holes with a radial interval of 5 mm. Every hole has a 0.5 mm radial width, 3 mm depth and 15° poloidal opening angle, as illustrated in Fig. 2. At the end of the hole, the graphite collector surrounds the back surface of hole, aiming to collect all the particles there. When the DEP is working, a

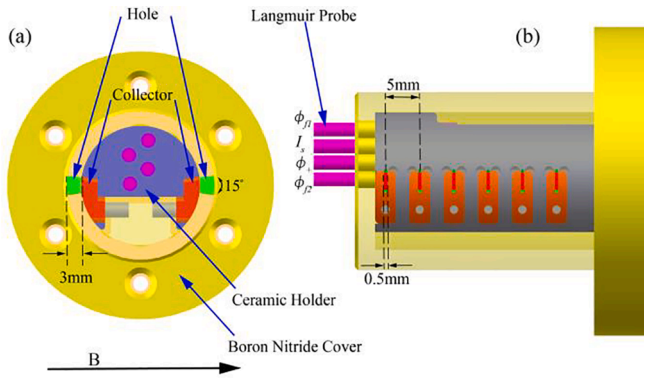

Fig. 2. (a) Front view of DEP with the boron nitride cover shown in translucence; (b) right side view of DEP, the signal names of the four Langmuir probe pins are labelled.

positive biasing voltage + 180 V is applied to the graphite collector, with the vacuum vessel wall as the circuit ground. In the edge plasma of tokamak and stellarator, the ion and electron temperatures are typically from several electron volts to 100 eV, as measured by Langmuir probe, RFA and ion sensitive probe [18,29–32]. Under this setup of DEP, the low energy ions are repelled by the positive biasing voltage, and most of the high energy ions are blocked by the hole surface due to their large ion Larmor radius and small hole width. In consequence, the collected current is mainly contributed by electrons, and the current difference between the two opposite collectors signifies the current driven by unidirectional electrons. The validity and rationality of DEP has been demonstrated by a particle orbit simulation [33], revealing that the contribution of ions to the collected current could be ignored if compared with that from electrons. This radially DEP array could measure the spatial structure and amplitude of the unidirectional electron current.

The boron nitride has a small outer diameter of 26 mm and an inner diameter of 20 mm, for the purpose of aligning the two opposite DEP channels along the same magnetic flux tube. The signal names of the DEP are shown in Fig. 3 and Fig. 4, with channels 1–6 located on the right side and channels 7–12 located on the left side when viewed from the center of tokamak. In our experiment, the toroidal magnetic field is along the clockwise direction viewed from top, while the plasma current is in the anti-clockwise direction. The Langmuir probe tip has a diameter of 2 mm and protrudes 4 mm from the boron nitride cover. The arrangement and signal names of the Langmuir probe is illustrated in Fig. 2 (b) and Fig. 4. It should be pointed out that the LP pins have a certain poloidal gap among them to avoid the blocking effect of

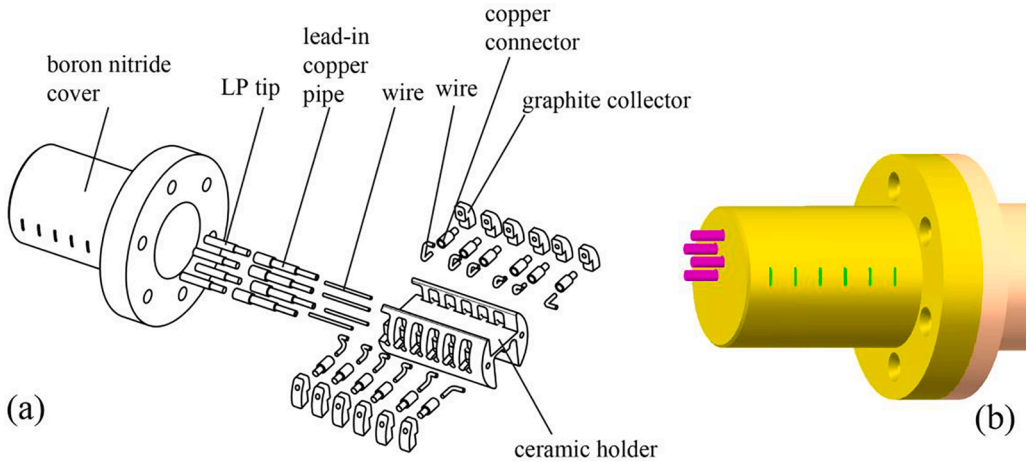

Fig. 1. Sketch of DEP. (a) Exploded drawing; (b) side view.

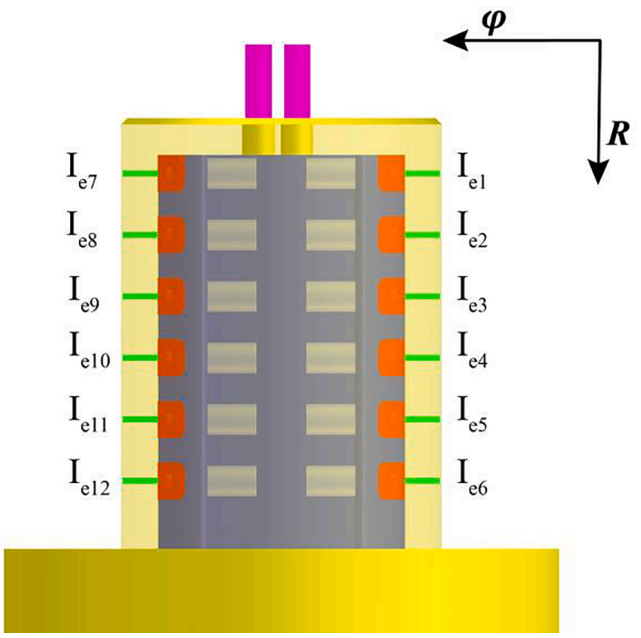

Fig. 3. Bottom view of DEP. The signal names of the DEP channels are labelled.

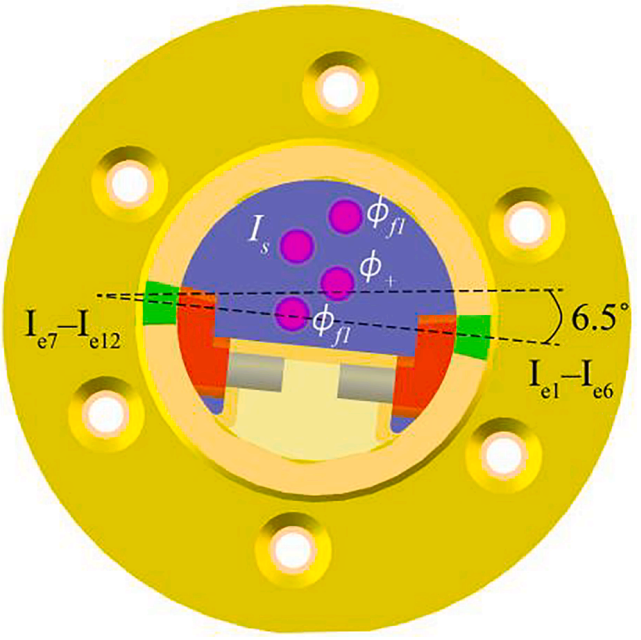

Fig. 4. The front view of DEP which is rotated by 6.5° clockwise in experiment.

magnetic field line. The sampling rate of the reciprocating probe system is 1 MHz in our experiment.

Experimental results

In this section, the commissioning of DEP is given in section 3.1 by sweeping the biasing voltage of collector, and then the measurement of unidirectional electron current in LHW modulation experiment is presented in section 3.2. As calculated by the magnetic equilibrium code EFIT, the local magnetic field line has a tilted angle around 6.5°, therefore the probe head of DEP is rotated clockwise by 6.5° to match the local field line, as illustrated in Fig. 4, i.e., the connection line of two opposite channels aligns with the local magnetic field.

Commissioning of DEP

The characteristics of collector current I and biasing voltage V_b is obtained by sweeping V_b from −150 V to + 130 V. In this commissioning experiment, because only one AC power supply is available, channels 1 and 7 are operated in the swept voltage mode, while the other channels are biased with a DC voltage of + 180 V. The plasma parameters are stable when the reciprocating probe reaches its innermost position, with plasma current $I_p = 450$ kA, line-integrated density $n_{el} = 5 \times 10^{19}$ m^{-2}, $q_{95} = 4$ and 4.6 GHz LHW heating power 1 MW. The temporal evolutions of biasing voltage and the corresponding collected current are shown in Fig. 5, with a swept frequency of 500 Hz. At the innermost position, the major radius of channels 1 and 7 is $R = 2337$ mm, which is about 25 mm outside the last closed flux surface (LCFS). When the biasing voltage is negative enough, the collected currents are close to zero for both channels. With the increase of biasing voltage, the absolute value of collected current increases significantly. It should be pointed out that in both the V_b ramp-up and ramp-down phases, the collected currents of both channels have symmetrical shape about the minimum of V_b, though there are some fluctuations in the signals. Note that the negative collected current I_e means that the collected electron current is larger than the ion current, while the positive current I_e signifies that the ion current is larger than the electron current. In the positive range of V_b, the current I_{e7} (left channel) is clearly larger than the current I_{e1} (right channel), revealing significant difference between the two opposite directions.

The $I-V$ characteristics of both channels are presented in Fig. 6, with the raw signal data from 5.76 s to 5.77 s (5 cycles). Typically, an exponential decay function is used to fit the classic $I-V$ curve. Here we use the following formula to fit the data in Fig. 6:

$$I(V) = I_{01} + I_{02}\left[1 - e^{-\frac{(V-V_0)}{V_a}}\right] H(V - V_0) \tag{1}$$

$$H(x) = \begin{cases} 0, x < 0 \\ 1, x \geq 0 \end{cases} \tag{2}$$

$H(x)$ is the Heaviside step function. In Eq. (1), the collected current I_{01} (when V_b is negative enough) and I_{02} (when V_b is positive enough) are

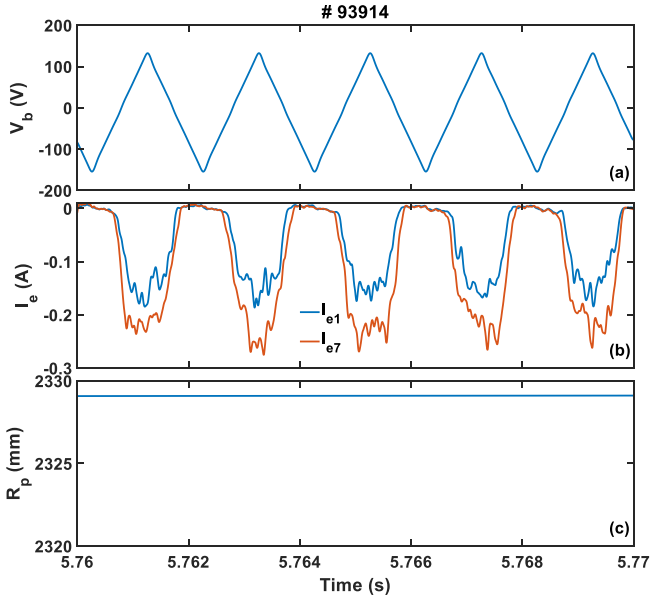

Fig. 5. Temporal traces of swept biasing voltage (a) and the corresponding collected current (b) of DEP. The radial position of reciprocating probe is shown in (c).

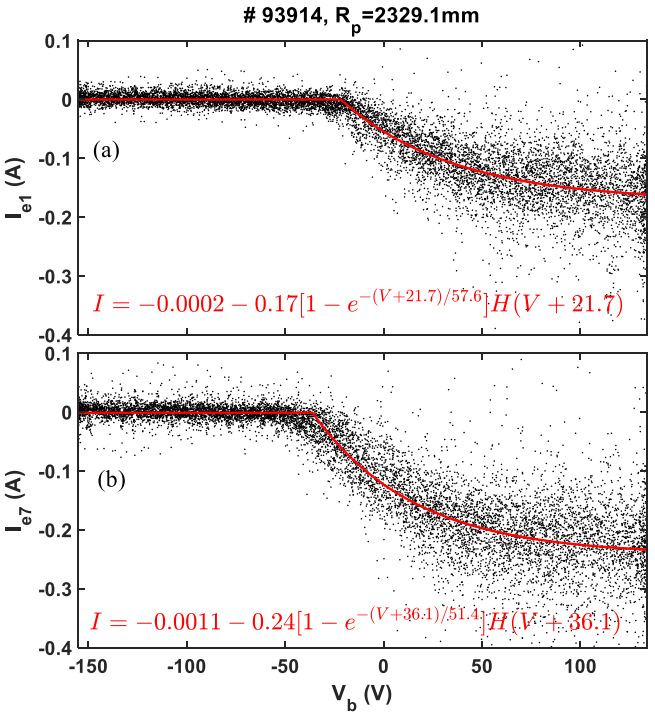

Fig. 6. *I-V* characteristics for DEP channel 1 (a) and channel 7 (b) at the innermost position of reciprocating probe. In each panel, the experimental data is fitted by Eq. (1).

used to illustrate the current asymmetry between the upstream and downstream sides. The fitted curve from Eq. (1) is shown in Fig. 6, and the corresponding fitted functions is also annotated. For both channels 1 and 7, the collected current is close to zero when $V < V_0$, then current I_e obeys the exponential decay function but with an offset. When fitted by Eq. (1), in contrast with the right channel 1, the left channel 7 has more negative threshold voltage V_0 and larger amplitude of I_{02}. It is an important feature that $I_{01} \approx 0$ when $V < V_0$, indicating that the ion current received by the graphite collector is almost equal to the electron current from high energy electrons which can overcome the negative biasing voltage. The left channel 7 has a bit larger I_{01} than the right channel, signifying that the unidirectional electrons are mainly from the left side. In the current exponential decay region ($V > V_0$), the electron current increases with V_b, while the ion current decreases with V_b. When $V_b > V_a$, the collected current gets saturated gradually, indicating that it is necessary to bias the graphite collector to enough high positive value, i.e., +180 V in the following experiment. It should be pointed out that the collected current still increases slightly when $V > +100$ V, which is similar with the increases of collected electron current of a typical Langmuir probe when the biasing voltage is positive [34]. A possible reason for this current slight increase is the expansion of magnetic flux tube when the biasing voltage is positive enough, consequently the electrons in the adjacent flux tube are collected and the slight increases of current with the positive biasing voltage is observed [35]. Besides, the current difference between the two opposite channels 1 and 7 is obvious when V_b is positive, indicating the asymmetry of unidirectional electron current caused by LHW. According to the particle orbit simulation of DEP [33], the currents contributed by thermal electrons which obey the Maxwell-Boltzmann velocity distribution from two opposite DEP channels almost equal to each other, therefore the obvious net current between these two channels is mainly caused by unidirectional electrons.

Note that in our data analysis the effects of secondary electron emission (SEE) and electron back-scattering (EBS) are not taken into account. According to some previous works in modelling and experiment, the coefficients of SEE and EBS are low when the incident energy is a few tens of electron volts, but increases significantly when the incident energy reaches several hundreds of electron volts [36,37]. Note that the incident electrons are accelerated when the biasing voltage of the graphite collector is $V_b = +180$ V, leading to a raise of the incident energy of electrons. In this condition, the electron temperature generated by SEE in general is very small, and these electrons have no impact on the collected current since they will flow back to the collector. While the EBS could produce electrons with a fraction of incident energy, and some superthermal electrons could be generated since the energy of incident electrons increases significantly in this acceleration process, which would affect the collected current. If there is a considerable component of superthermal electrons, the effects of SEE, EBS or photoemission could play an important role and should be taken into consideration in the interpretation of DEP data. As seen in Fig. 6, the DEP collected current is close to zero when V_b is negative enough (below −80 V), indicating that the component of superthermal electrons which have very high temperature can be negligible in this experiment.

SOL unidirectional electron current induced by LHW

Since LHW has the ability to drive unidirectional electrons in the edge plasma of tokamak [14], a series of experiment has been carried out in EAST to measure these unidirectional electron currents in the plasma edge. The typical radial profile of the LHW induced SOL current is given in a LHW modulation experiment. In this discharge, the plasma current is $I_p = 400$ kA, line-integrated density $n_{el} = 3.5 \times 10^{19}$ m^{-2} and $q_{95} = 6.2$. The 4.6 GHz LHW heating power is set at 0.7 MW and modulated at 10 Hz with a 50% duty cycle, as shown in Fig. 7 (a). The reciprocating probe reaches its innermost position $R = 2315$ mm (with $R_{LCFS} = 2305$ mm) and stays there for 500 ms. All the DEP collectors are biased to + 180 V. When the LHW is switched off, the asymmetry of collected current from two opposite DEP channels is very weak, and the current amplitude $|I_e|$ is very small, as shown in Fig. 7 (b-g). When the LHW is turned on, the collected currents increase significantly in all DEP channels, but I_e in the left channels 8–12 is much larger than that of the corresponding right channels 2–6. However, in the first radial location

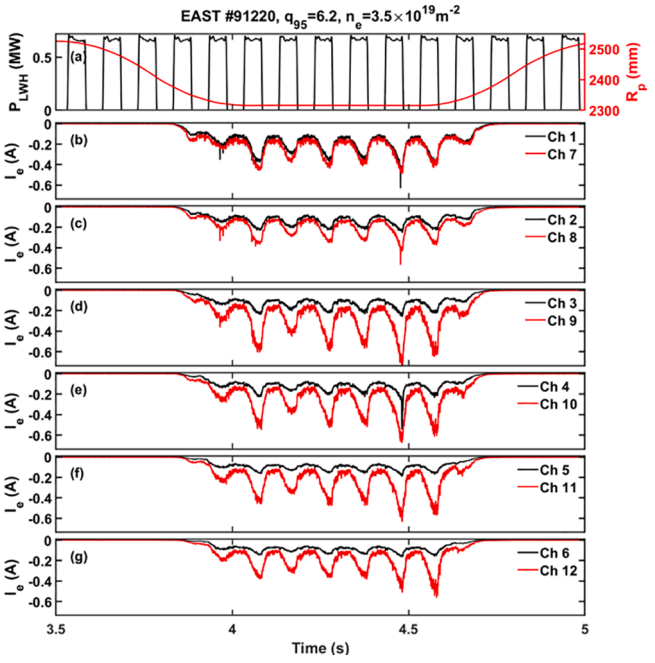

Fig. 7. Temporal evolution of plasma parameters. (a) LHW heating power and radial position of DEP; (b) DEP collected current of channels 1 and 7; (c) 2 and 8; (d) 3 and 9; (e) 4 and 10; (f) 5 and 11; (g) 6 and 12. The biasing voltage of DEP channels is + 180 V.

of the DEP array, I_{e1} and I_{e7} are basically symmetric in both LHW-on and LHW-off phases. Note that the signals are calibrated by assuming that the collected currents I_e are the same in the far-SOL region ($R =$ 2345 −2350 mm, with $R_{limiter} = 2350$ mm) in an Ohmic discharge on the same experimental day. The temporal evolution of DEP collected current confirms the existence of unidirectional electron current during the LHW-on phase. The electron temperature T_e and density n_e measured by the front four-tip probe also increase significantly during the LHW-on phase, while the floating potential becomes much more negative.

The net current is obtained by taking the difference of two opposite DEP channels, $I_{net} = I_{right} - I_{left}$, with channels 1–6 on right and 7–12 on left, as illustrated in Fig. 3 and Fig. 4. As predicted in the particle orbit simulation [33], the effective collected area of each channel is $S_{eff} = S_0/1.276$, where $S_0 = 1.9$ mm^2 is the area of the DEP front surface. Consequently, the net current density can be derived from $j_{net} = I_{net}/S_{eff}$, as presented in Fig. 8. The net current density is very small in the LHW-off phase, while a strong enhancement of j_{net} can be found in the LHW-on phase. The direction of the SOL unidirectional electron current driven by LHW is in the anti-clockwise direction viewed from top, which has the same direction as the plasma current I_p. As mentioned in section 3.1, the component of superthermal electrons is very small in our LHW heating experiment, and this net current is mainly contributed by the unidirectional electrons. As indicated by the $I-V$ curve in Fig. 6, the temperature of these unidirectional electrons is not too high because they can be repelled by enough negative biasing voltage (-80 V). With these electrons, a plasma flow and current could be formed during the LHW-on phase. Note that the non-zero net current during LHW-off phase indicates the existence of parallel flow, though it is much weaker than that in the LHW-on phase. The radial profiles of net current during both LHW-on and LHW-off phases are shown in Fig. 8 (b). The LHW induced SOL current peaks at $R \approx 2335$ mm, covers a wide radial region of over 20 mm ($R > 2330$), with its maximum about 20 A/cm^2, and decreases gradually when approaching the LCFS. Note that this SOL current is mainly driven by unidirectional electrons induced by LHW, which should be distinguished from the natural SOL current, such as

the Pfirsch-Schlüter (PS) current driven by the radial electric field and radial gradient of pressure [38]. In addition, the PS current is contributed by both electrons and ions [39,40], and the SOL ion flow velocity measured by Mach probe in many tokamaks is roughly consistent with the magnitude and direction of PS flow [41–43]. Considering the poloidal elongation of filament (or eddy), and according to the previous LHW current model [16], a poloidal length of 10 cm is assumed for this LHW induced current filament. Therefore, the estimated current of each LHW filament could be about $I_{total} = \pi \times 1\text{cm} \times 5\text{cm} \times 18\text{A/cm}^2 = 282$ A, which is consistent with the previous modelling where the total SOL current caused by 5 LHW antennas is around 1–1.5 kA [16,17,44]. In Alcator C-Mod, the peak SOL parallel current density induced by LHW could be up to 60 A/cm^2 at line averaged density $n_e = 1.2 \times 10^{20}$ m^{-3} [14]. Since the line averaged density in EAST is much lower than that in Alcator C-Mod, a smaller current density of LHW filament in EAST is in line with expectations. Besides, the LHW SOL current is along the plasma current direction in both EAST and Alcator C-Mod.

Summary

A newly directional electron probe has been developed on EAST to directly measure the edge current driven by unidirectional electrons. The DEP consists of two radial arrays of channels which have opposite directions and align along the local magnetic field. Each radial array has 6 channels with a radial interval of 5 mm. Every channel has a hole with 0.5 mm radial width, 3 mm depth and 15° poloidal opening angle. At the end of the DEP hole, a graphite collector is biased to positive potential to repel low energy ions and collect electrons. Since the high energy ions have Larmor radii which are larger than the radial width of DEP hole, most of them will be blocked by the hole surface. Therefore, the DEP collected current is mainly contributed by electrons. Because the two opposite DEP channels are tilted to align with the local magnetic field, the current difference between these two channels is the unidirectional electron current in the flux tube. The radial DEP array could be used to measure the amplitude and structure of unidirectional electron current. In the commissioning experiment of DEP, the graphite collector is swept from −150 V to + 130 V, and the collected current is close to zero when the biasing voltage is smaller than a negative threshold, indicating that very few ions can penetrate the DEP hole and be collected by the graphite collector. In the LHW modulation experiment, the collected currents of DEP channels are very small during the LHW-off phase, while during the LHW-on phase the collected currents increase significantly

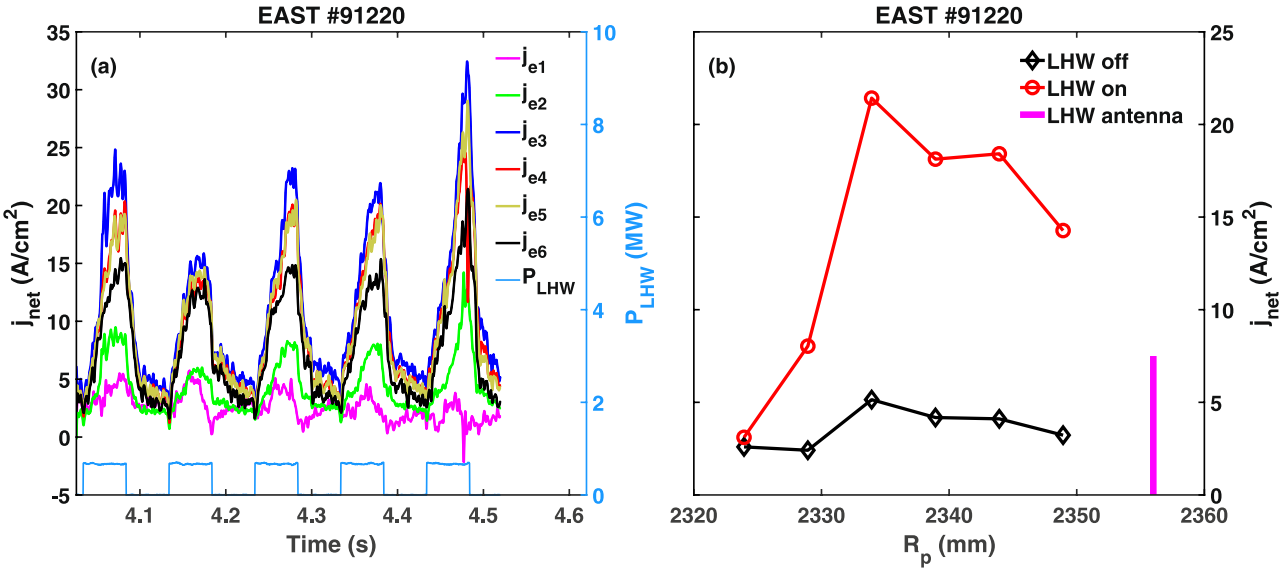

Fig. 8. (a) Temporal evolution of net current density of DEP and the LHW heating power; (b) radial profiles of net current density measured at the innermost position of DEP in both LHW-on and LHW-off phases. Positive j_{net} signifies the net current along the anti-clockwise direction viewed from top. The radial position of 4.6 GHz LHW antenna is marked in magenta vertical line. (For interpretation of the references to colour in this figure legend, the reader is referred to the web version of this article.)

and exhibit a strong asymmetry between two opposite channels in a wide radial region, demonstrating the existence of unidirectional electron current induced by LHW. This LHW induced current covers a radial region of over 20 mm, and decreases to very low value near the LCFS. This unidirectional electron current is along the direction of plasma current, which is the same as that in Alcator C-Mod. The peak current density is about 20 A/cm^2, which is also in the same magnitude as that in Alcator C-Mod. The estimated LHW filament current agrees with the previous modelling in both the amplitude and radial structure. More dedicated study of the LHW induced filament current will be performed based on this newly developed DEP on EAST, including its dependence on the plasma density, edge magnetic topology and heating power. In this paper, it is important to commission this DEP array in experiment, which could directly measure the unidirectional electron current in the edge of magnetically confined plasmas with high temporal resolution. The DEP array has huge potential on the edge physics study, such as the SOL current driven by RF waves and ELM filament dynamics.

CRediT authorship contribution statement

S.C. Liu: Methodology, Data curation, Formal analysis. **Y. Liang:** Conceptualization. **N. Yan:** Resources. **L. Liao:** Investigation. **W.Y. Wei:** Investigation. **L.Y. Meng:** Investigation. **L. Chen:** Investigation. **S. Xu:** Investigation. **N. Zhao:** Investigation. **R. Chen:** Investigation. **G.H. Hu:** Investigation. **Y.L. Li:** Investigation. **X.J. Liu:** Funding acquisition. **T.F. Ming:** Investigation. **Y. Sun:** Funding acquisition. **J.P. Qian:** Funding acquisition. **L. Zeng:** Funding acquisition. **G.Q. Li:** Funding acquisition. **L. Wang:** Funding acquisition. **G.S. Xu:** Funding acquisition. **X.Z. Gong:** Supervision. **X. Gao:** Supervision.

Declaration of Competing Interest

The authors declare that they have no known competing financial interests or personal relationships that could have appeared to influence the work reported in this paper.

Acknowledgement

This work was supported by the National Natural Science Foundation of China (Nos. 11875294, 11875292, 11922513, U19A20113 and 119 75271), the National MCF Energy R&D Program (Nos. 2017YFE0301100, 2019YFE03040000, 2019YFE03030000 and 2017YFE0301300), and the Users with Excellence Program of Hefei Science Center, CAS under grant Nos. 2021HSC-UE014.

References

[1] S.J. Zweben, D.P. Stotler, J.L. Terry, B. LaBombard, M. Greenwald, M. Muterspaugh, C.S. Pitcher, K. Hallatschek, R.J. Maqueda, B. Rogers, J. L. Lowrance, V.J. Mastrocola, G.F. Renda, Edge turbulence imaging in the Alcator C-Mod tokamak, Phys. Plasmas 9 (5) (2002) 1981–1989.

[2] S. Zoletnik, G. Anda, C. Biedermann, A.D. Carralero, G. Cseh, D. Dunai, C. Killer, G. Kocsis, A. Krämer-Flecken, M. Otte, B. Shanahan, T. Szepesi, M. Vecsei, L. Zsuga, Multi-diagnostic analysis of plasma filaments in the island divertor, Plasma Phys. Control. Fusion. 62 (1) (2020) 014017, https://doi.org/10.1088/1361-6587/ab5241.

[3] D.A. D'Ippolito, J.R. Myra, S.J. Zweben, Convective transport by intermittent blob-filaments: Comparison of theory and experiment, Phys. Plasmas 18 (6) (2011) 060501, https://doi.org/10.1063/1.3594609.

[4] A. Kirk, H.R. Wilson, R. Akers, N.J. Conway, G.F. Counsell, S.C. Cowley, J. Dowling, B. Dudson, A. Field, F. Lott, B. Lloyd, R. Martin, H. Meyer, M. Price, D. Taylor, M. Walsh, T.MAST. team, Structure of ELMs in MAST and the implications for energy deposition, Plasma Phys. Control. Fusion. 47 (2) (2005) 315–333.

[5] F. Militello, N.R. Walkden, T. Farley, W.A. Gracias, J. Olsen, F. Riva, L. Easy, N. Fedorczak, I. Lupelli, J. Madsen, A.H. Nielsen, P. Ricci, P. Tamain, J. Young, Multi-code analysis of scrape-off layer filament dynamics in MAST, Plasma Phys. Control. Fusion. 58 (10) (2016) 105002, https://doi.org/10.1088/0741-3335/58/10/105002.

[6] N. Vianello, V. Naulin, R. Schrittwieser, H.W. Müller, M. Zuin, C. Ionita, J. J. Rasmussen, F. Mehlmann, V. Rohde, R. Cavazzana, M. Maraschek, Direct Observation of Current in Type-I Edge-Localized-Mode Filaments on the ASDEX Upgrade Tokamak, Phys. Rev. Lett. 106 (12) (2011), https://doi.org/10.1103/PhysRevLett.106.125002.

[7] H.W. Müller, J. Adamek, R. Cavazzana, G.D. Conway, C. Fuchs, J.P. Gunn, A. Herrmann, J. Horaček, C. Ionita, A. Kallenbach, M. Kočan, M. Maraschek, C. Maszl, F. Mehlmann, B. Nold, M. Peterka, V. Rohde, J. Schweinzer, R. Schrittwieser, N. Vianello, E. Wolfrum, M. Zuin, Latest investigations on fluctuations, ELM filaments and turbulent transport in the SOL of ASDEX Upgrade, Nucl. Fusion 51 (7) (2011) 073023, https://doi.org/10.1088/0029-5515/51/7/073023.

[8] N.J. Fisch, Confining a Tokamak Plasma with Rf-Driven Currents, Phys. Rev. Lett. 41 (13) (1978) 873–876.

[9] R. Cesario, L. Amicucci, C. Castaldo, M. Kempenaars, S. Jachmich, J. Mailloux, O. Tudisco, A. Galli, A. Krivska, Plasma edge density and lower hybrid current drive in JET (Joint European Torus), Plasma Phys. Control. Fusion. 53 (8) (2011) 085011, https://doi.org/10.1088/0741-3335/53/8/085011.

[10] Y. Neyatani, Improved confinement with plasma profile and shape controls in JT-60U, Plasma Phys. Control. Fusion. 38 (12A) (1996) A181–A191.

[11] J.R. Wilson, R. Parker, M. Bitter, P.T. Bonoli, C. Fiore, R.W. Harvey, K. Hill, A. E. Hubbard, J.W. Hughes, A. Ince-Cushman, C. Kessel, J.S. Ko, O. Meneghini, C. K. Phillips, M. Porkolab, J. Rice, A.E. Schmidt, S. Scott, S. Shiraiwa, E. Valeo, G. Wallace, J.C. Wright, Lower hybrid heating and current drive on the Alcator C-Mod tokamak, Nucl. Fusion 49 (11) (2009) 115015, https://doi.org/10.1088/0029-5515/49/11/115015.

[12] M.H. Li, B.J. Ding, J.Z. Zhang, K.F. Gan, H.Q. Wang, Y. Peysson, J. Decker, L. Zhang, W. Wei, Y.C. Li, Z.G. Wu, W.D. Ma, H. Jia, M. Chen, Y. Yang, J.Q. Feng, M. Wang, H.D. Xu, J.F. Shan, F.K. Liu, Study on lower hybrid current drive efficiency at high density towards long-pulse regimes in Experimental Advanced Superconducting Tokamak, Phys. Plasmas 21 (6) (2014) 062510, https://doi.org/10.1063/1.4883640.

[13] Lu B. et al Recent LHCD experiments on HL-2A and LHCD system development on HL-2M, 23rd Topical Conference on Radiofrequency Power in Plasmas 2254 (2020) 030008.

[14] G.M. Wallace, R.R. Parker, P.T. Bonoli, A.E. Hubbard, J.W. Hughes, B. L. LaBombard, O. Meneghini, A.E. Schmidt, S. Shiraiwa, D.G. Whyte, J.C. Wright, S.J. Wukitch, R.W. Harvey, A.P. Smirnov, J.R. Wilson, Absorption of lower hybrid waves in the scrape off layer of a diverted tokamak, Phys. Plasmas 17 (8) (2010) 082508, https://doi.org/10.1063/1.3465662.

[15] Y. Liang, X.Z. Gong, K.F. Gan, E. Gauthier, L. Wang, M. Rack, Y.M. Wang, L. Zeng, P. Denner, A. Wingen, B. Lv, B.J. Ding, R. Chen, L.Q. Hu, J.S. Hu, F.K. Liu, Y.X. Jie, J. Pearson, J.P. Qian, J.F. Shan, B. Shen, T.H. Shi, Y. Sun, F.D. Wang, H.Q. Wang, M. Wang, Z.W. Wu, S.B. Zhang, T. Zhang, X.J. Zhang, N. Yan, G.S. Xu, H.Y. Guo, B. N. Wan, J.G. Li, Magnetic Topology Changes Induced by Lower Hybrid Waves and their Profound Effect on Edge-Localized Modes in the EAST Tokamak, Phys. Rev. Lett. 110 (23) (2013), https://doi.org/10.1103/PhysRevLett.110.235002.

[16] M. Rack, L. Zeng, P. Denner, Y. Liang, A. Wingen, K.F. Gan, L. Wang, F.K. Liu, B. Shen, B.N. Wan, J.G. Li, Modelling of LHW-induced helical current filaments on EAST: study of an alternative method of applying RMPs, Nucl. Fusion 54 (6) (2014) 064016, https://doi.org/10.1088/0029-5515/54/6/064016.

[17] S. Xu, M. Rack, Y. Liang, J. Huang, M. Jia, Y. Feng, J. Cosfeld, H. Zhang, S. Liu, Y. Gao, K. Gan, W. Feng, L. Wang, W. Zholobenko, D. Reiter, First three-dimensional edge plasma transport simulations with magnetic perturbations induced by lower hybrid waves on EAST, Nucl. Fusion 58 (10) (2018) 106008, https://doi.org/10.1088/1741-4326/aad296.

[18] M. Henkel, Y. Li, Y. Liang, P. Drews, A. Knieps, C. Killer, D. Nicolai, D. Höschen, J. Geiger, C. Xiao, N. Sandri, G. Satheeswaran, S. Liu, O. Grulke, M. Jakubowski, S. Brezinsek, M. Otte, O. Neubauer, B. Schweer, G. Xu, J. Cai, Retarding field analyzer for the wendelstein 7-X boundary plasma, Fusion Eng. Des. 157 (2020) 111623, https://doi.org/10.1016/j.fusengdes.2020.111623.

[19] M. HENKEL, D. HÖSCHEN, Y. LIANG, Y. LI, S.C. LIU, D. NICOLAI, N. SANDRI, G. SATHEESWARAN, N. YAN, H.X. ZHANG, Multi-channel retarding field analyzer for EAST, Plasma Sci. Technol. 20 (5) (2018) 054001, https://doi.org/10.1088/2058-6272/aab490.

[20] S.J. Stephanakis W.H. Bennett 18 1 1969 27 31.

[21] J.C. Ingraham, R.F. Ellis, J.N. Downing, C.P. Munson, P.G. Weber, G.A. Wurden, Energetic electron measurements in the edge of a reversed-field pinch, Phys. Fluids. B 2 (1) (1990) 143–159.

[22] Y. Yagi, V. Antoni, M. Bagatin, D. Desideri, E. Martines, G. Serianni, F. Vallone, Measurement of superthermal electron flow and temperature in a reversed-field pinch experiment by an electrostatic electron energy analyser, Plasma Phys. Control. Fusion. 39 (11) (1997) 1915–1927.

[23] J. Zhang, Z.Y. Shang, E.Y. Wang, Z.H. Wang, L.B. Ran, H.R. Yang, K.Q. Huang, X. M. Liu, S.J. Qian, Experimental-Study in the Edge Plasma of the Hl-1 Tokamak with a Mach Probe and a Directional Probe, J. Nucl. Mater. 220-222 (1995) 717–720.

[24] R. Jones, Directional Probe for Analysis of Energetic Plasma Electrons, Am J Phys 46 (1978) 1192.

[25] Tsumori K. et al Polar distribution of Ions and Electrons in Extraction Region of a Large-Scaled Caesium Seeded Ion Source, Third International Symposium on Negative Ions, Beams and Sources (Nibs 2012) 1515 (2013) 149.

[26] M. Rack, Y. Liang, H. Jaegers, J. Aßmann, G. Satheeswaran, Y. Xu, J. Pearson, Y. Yang, P. Denner, L. Zeng, A rotating directional probe for the measurements of fast ion losses and plasma rotation at Tokamak Experiment for Technology Oriented Research, Rev. Sci. Instrum. 84 (8) (2013) 083501, https://doi.org/10.1063/1.4816821.

[27] S. Kado, et al., Plasma mow measurements in linear divertor simulator MAP-H using Mach Probe and Directional Langmuir Probe, Contrib. Plasm. Phys. 44 (2004) 656.

[28] T. Shikama, S. Kado, A. Okamoto, S. Kajita, S. Tanaka, Practical formula for Mach number probe diagnostics in weakly magnetized plasmas, Phys. Plasmas 12 (4) (2005) 044504, https://doi.org/10.1063/1.1872895.
[29] P. Drews C. Killer J. Cosfeld A. Knieps S. Brezinsek M. Jakubowski C. Brandt S. Bozhenkov A. Dinklage J. Cai M. Endler K. Hammond M. Henkel Y. Gao J. Geiger O. Grulke D. Höschen R. König A. Krämer-Flecken Y. Liang Y. Li S. Liu H. Niemann D. Nicolai O. Neubauer U. Neuner M. Rack K. Rahbarnia L. Rudischhauser N. Sandri G. Satheeswaran S. Schilling H. Thomsen T. Windisch S. Sereda 19 2019 179 183.
[30] Y.L. Li, G.S. Xu, C. Xiao, H.Q. Wang, N. Yan, B.N. Wan, L. Chen, Y.L. Liu, H. Zhang, W. Zhang, L. Wang, G.H. Hu, R. Chen, J.C. Xu, Y. Ye, J. Li, Retarding field analyzer for the EAST plasma boundary, Rev. Sci. Instrum. 87 (12) (2016) 123503, https://doi.org/10.1063/1.4971317.
[31] N. Ezumi, S. Masuzaki, N. Ohno, Y. Uesugi, S. Takamura, LHD Experimental Group, Ion temperature measurement using an ion sensitive probe in the LHD divertor plasma, J. Nucl. Mater. 313-316 (2003) 696–700.
[32] M. Kočan, F.P. Gennrich, A. Kendl, H.W. Müller, Ion temperature fluctuations in the ASDEX Upgrade scrape-off layer, Plasma Phys. Control. Fusion. 54 (8) (2012) 085009, https://doi.org/10.1088/0741-3335/54/8/085009.
[33] Liu S.C. et al Modelling and application of a new method to measure the non-thermal electron current in the edge of magnetically confined plasma, Nucl. Fusion (2021) accepted.
[34] D.E. Post, et al., Physics of plasma-wall interactions in controlled fusion, New York, Plenum Press, 1986, p. 144.
[35] P.C. Stangeby, Determination of T-e from a Langmuir probe in a magnetic field by directly measuring the probe's sheath drop using a pin-plate probe, Plasma Phys. Control. Fusion. 37 (11) (1995) 1337–1347.
[36] P. Tolias, M. Komm, S. Ratynskaia, A. Podolnik, Origin and nature of the emissive sheath surrounding hot tungsten tokamak surfaces, Nuclear Materials and Energy 25 (2020) 100818, https://doi.org/10.1016/j.nme.2020.100818.
[37] J.P. Gunn, Evidence for strong secondary electron emission in the tokamak scrape-off layer, Plasma Phys. Control. Fusion. 54 (8) (2012) 085007, https://doi.org/10.1088/0741-3335/54/8/085007.
[38] M.J. Schaffer, A.V. Chankin, H.Y. Guo, G.F. Matthews, R. Monk, Pfirsch-Schluter currents in the jet divertor, Nucl. Fusion 37 (1) (1997) 83–99.
[39] P.C. Stangeby, The plasma boundary of magnetic fusion devices, Bristol, Institute of Physics Publishing, 2000, p. 561.
[40] J.D. Treffert, et al., Measurement of the Pfirsch-Schluter and Bootstrap Currents in a Stellarator, Phys. Rev. Lett. 53 (1984) 2409.
[41] N. Asakura, S. Sakurai, M. Shimada, Y. Koide, N. Hosogane, K. Itami, Measurement of natural plasma flow along the field lines in the scrape-off layer on the JT-60U divertor tokamak, Phys. Rev. Lett. 84 (14) (2000) 3093–3096.
[42] S.K. Erents, A.V. Chankin, G.F. Matthews, P.C. Stangeby, Parallel flow in the JET scrape-off layer, Plasma Phys. Control. Fusion. 42 (8) (2000) 905–915.
[43] S.C. Liu, H.Y. Guo, L. Wang, H.Q. Wang, K.F. Gan, T.Y. Xia, G.S. Xu, X.Q. Xu, Z. X. Liu, L. Chen, N. Yan, W. Zhang, R. Chen, L.M. Shao, S. Ding, G.H. Hu, Y.L. Liu, N. Zhao, Y.L. Li, X.Z. Gong, X. Gao, Effects of heating power on divertor in-out asymmetry and scrape-off layer flow in reversed field on Experimental Advanced Superconducting Tokamak, Phys. Plasmas 21 (12) (2014) 122514, https://doi.org/10.1063/1.4904205.
[44] S. Xu, M. Rack, Y. Liang, M. Jia, D. Reiter, Y. Feng, J. Cosfeld, Y. Sun, L. Wang, W. Feng, S. Liu, B. Zhang, X.L. Zou, J. Huang, J. Wu, J. Xu, L. Meng, Mechanism of the active divertor flux control by the supersonic-molecular-beam-injection with lower hybrid wave-induced magnetic perturbations on the EAST tokamak, Nucl. Fusion 60 (5) (2020) 056006, https://doi.org/10.1088/1741-4326/ab796a.